GMS-5 Satellite-Derived Cloud Properties Over the Tropical Western Pacific

M. L. Nordeen, D. R. Doelling, M. M. Khaiyer, and A. D. Rapp
Analytical Service and Materials, Inc.
Hampton, Virginia

P. Minnis and L. Nguyen
Atmospheric Sciences Division
National Aeronautics and Space Administration
Langley Research Center
Hampton, Virginia

Introduction

Satellite monitoring is used to supplement the paucity of surface data in the Tropical Western Pacific (TWP). By using satellite data, cloud properties and top-of-atmosphere broadband radiative fluxes can be derived and used for a variety of applications. In turn, these products may be used to develop a climatological base for the TWP. The focus of this study is to produce satellite-derived cloud properties over the TWP.

Data and Methodology

Hourly 5- and 1-km Geostationary Meteorological Satellite (GMS-5) visible (VIS) 0.65μm and infrared (IR) 11μm radiances, respectively, were analyzed using the layer bispectral threshold method (LBTM) of Minnis et al. (1995) to derive cloud and radiation properties. Three predetermined layers, low ($z < 2$ km), middle ($2 \text{ km} \leq z < 6$ km), and high ($z \geq 6$ km), are used to classify the cloud properties determined for each grid box and hour. Each pixel is classified as either clear or cloudy. A reflectance model that assumes an effective cloud droplet size of 10 μm is used to derive optical depth (OD) for low clouds while a hexagonal crystal model representing a cirrostratus size distribution is used to determine OD for mid-level and high clouds. Once OD is known, IR emissivity is calculated and used to adjust cloud-top temperatures for semi-transparent clouds. If the cloud is optically thick, cloud-top temperature and cloud center temperature are equivalent. If OD cannot be calculated, the cloud center temperature is set equal to the IR temperature or, for high clouds, it is set equal to the tropopause temperature and the emissivity and OD are computed. The temperatures are then converted to altitude using vertical profiles of temperature from the European Center for Medium-range Weather Forecasts (ECMWF) analyses.

The GMS VIS data were calibrated using the technique of Nguyen et al. (1999) based on a reference calibration of the Advanced Very High Resolution Radiometer (AVHRR) on National Oceanic and Atmospheric Administration (NOAA)-14. Shortwave (SW) broadband albedo and outgoing longwave

(LW) flux were derived from the VIS and IR data using narrow-to-broadband conversion functions based on matched 1986 Earth Radiation Budget Experiment (ERBE) and GMS data (Doelling et al. 1996). Albedos and LW fluxes were computed for both clear and cloudy conditions and used to determine the cloud radiative forcing for the period.

The cloud parameters were derived for each pixel and averaged on a 1° x 1° grid covering a domain extending from 10°N to 10°S and 130°E to 180° to obtain a large-scale characterization of the clouds in the TWP area. The results were also averaged on a 12 x 12 0.5° grid covering a domain extending from 2.75°N to 3.25°S and 163.25°E to 169.25°E. The middle box of this smaller grid is centered over Nauru to facilitate comparisons of the satellite results with surface observations taken during the Nauru99 Intensive Operational Period (IOP). Maps of clear-sky reflectance were produced for the 1° grid by finding the minimum reflectance for each pixel observed during the 1-month period for a given Universal Time Coordinates (UTC) hour. The clear-sky visible threshold is set equal to this value plus one standard deviation based on the variance of the minimum reflectance within the box.

The surface observations consist of cloud amounts derived from the Whole Sky Imager (WSI), the Micropulse Lidar (MPL), the Atmospheric Radiation Measurement (ARM) Millimeter Wave Cloud Radar (MMCR), and a Vaisala Ceilometer. These instruments were situated at the ARM surface site located on the leeward side of the island of Nauru. The cloud amounts were averaged for each UTC hour during the IOP for comparison with the satellite results.

Results

The Nauru99 IOP mean cloud properties for the TWP domain are shown in Figures 1 through 4. Total cloudiness (Figure 1) is greatest over the western half of the region corresponding to the vicinity of the warm pool. Low clouds are significant along the equator from 157°E to 167°E. Mid-level clouds are greatest over the southwestern half of the domain. High clouds, which can obscure low and mid-level clouds, are dominant over the western half of the domain where the mean high cloud cover exceeds 70 percent in some areas. Total cloud cover ranges from 43 to 80 percent with a mean value of 70 percent. Mean low-cloud OD (Figure 2) varies from 2 to 8 and is smallest over the northeastern corner. Maximum mid-level cloud OD is slightly higher, while high-cloud ODs are even more variable ranging from 1 to well over 10. Total cloud OD is greatest over the Tasmanian Sea and Indian Ocean with secondary maxima along the intertropical convergence zone (ITCZ) regime. Both total cloud amount and optical depth are at a minimum near Nauru. Figure 3 shows the mean clear and total IR temperatures and LW fluxes for the period. The clear IR and LW values are range between 294.0 and 294.3K and between 306 and 310 Wm^{-2}, respectively. The warmest values are found in an area of minimum cloudiness. The mean total IR and LW values vary from 260 to 290K and from 210 to 290 Wm^{-2}, respectively. The VIS and SW clear albedos for ocean (Figure 4) are in the expected ranges while the values over land are a bit higher than expected. These larger values are probably due to persistent cloud cover that precluded detection of the true clear-sky albedos. The total albedos mimic the high cloud amounts to some extent but are certainly influenced by the distribution of cloud ODs. The mean total albedo for the domain is 25 percent. Figure 5 shows the distribution of mean total cloud heights and thickness for the domain. The mean center cloud height refers to the radiating center and is always below the physical top of the cloud. The actual tops for cirrus clouds are generally around 2 km

higher than the center. The greatest mean heights correspond to the largest high cloud amounts. Estimates of mean cloud thickness vary from 1 to 4 km with the thickest clouds occurring in the areas with the most high cloud cover.

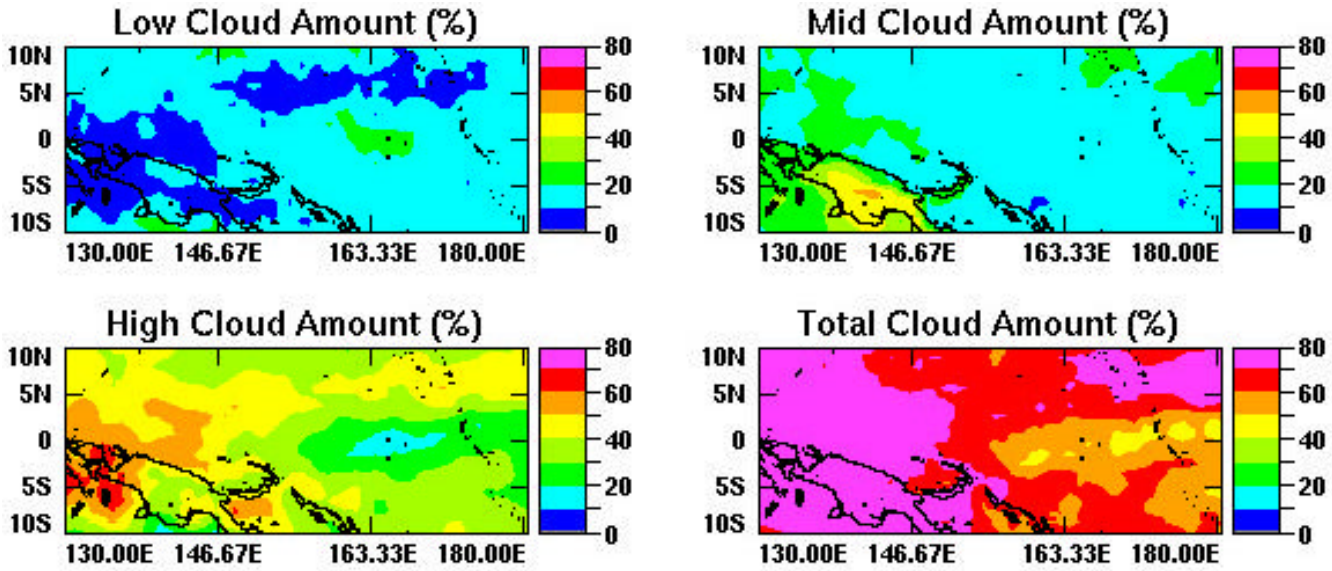

Figure 1. Mean cloud amounts derived from GMS-5 during Nauru99.

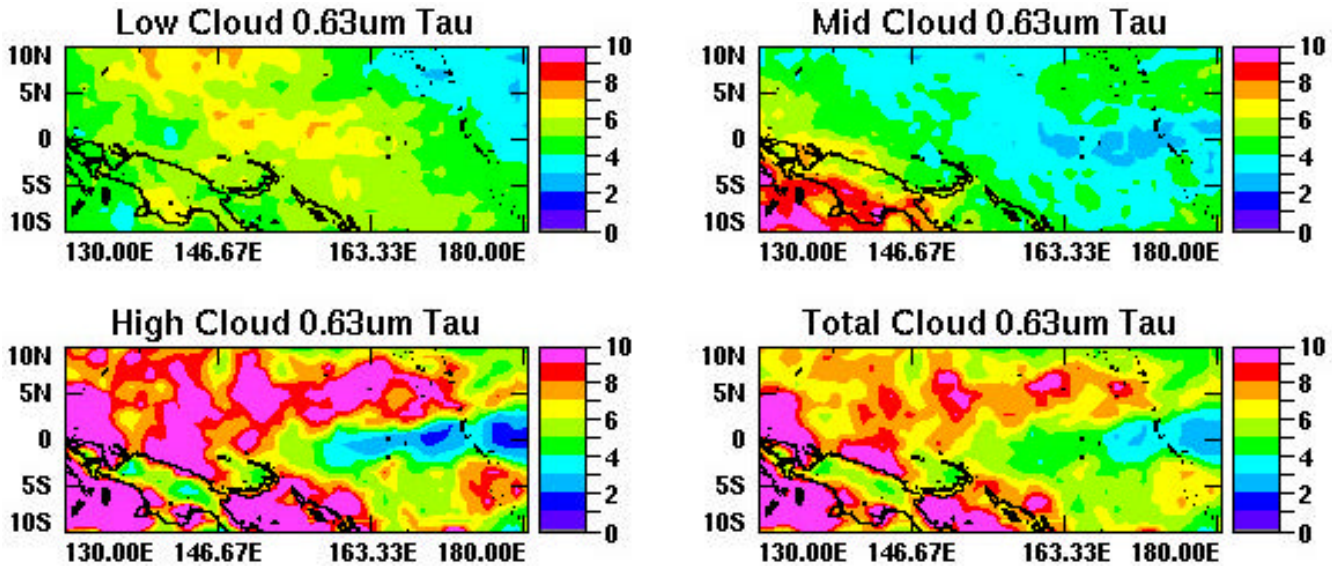

Figure 2. Mean cloud ODs derived from GMS-5 during Nauru99.

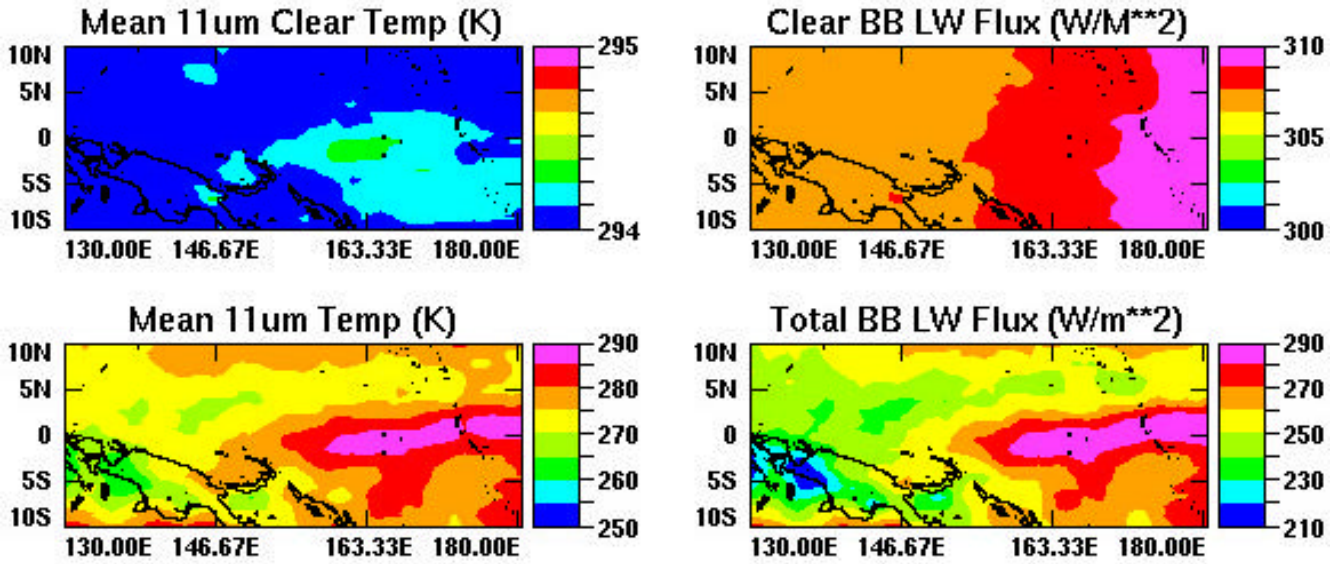

Figure 3. Mean IR temperatures and LW fluxes derived from GMs-5 during Nauru99.

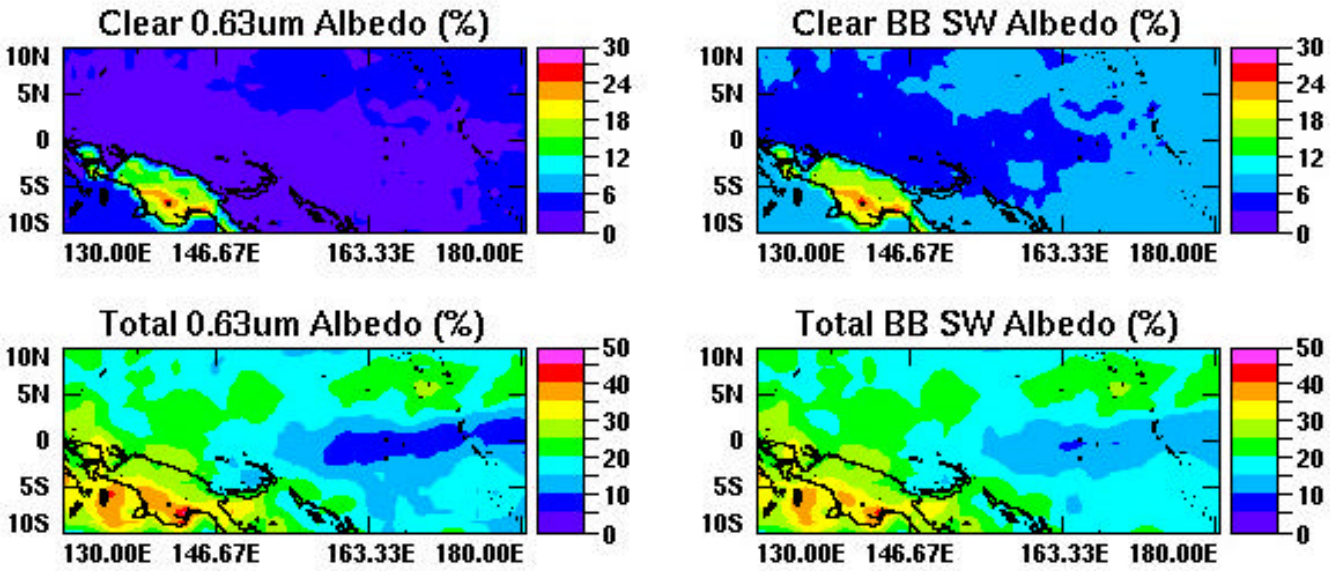

Figure 4. Mean cloud albedos derived from GMS-5 during Nauru99.

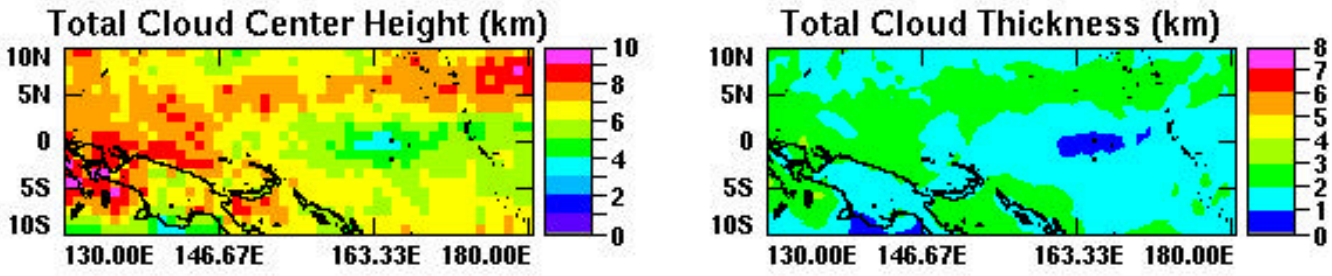

Figure 5. Mean total cloud parameters during Nauru99.

Cirrus clouds are defined here as high clouds with OD < 6. This definition does not include all of the cirrus clouds because some of them will overlap lower clouds such that the derived value of OD will exceed the threshold for cirrus clouds. Nevertheless, Figure 6 reveals that more than half of the high clouds are defined as cirrus. The mean ODs vary from 1 in the east to 3 over a few areas.

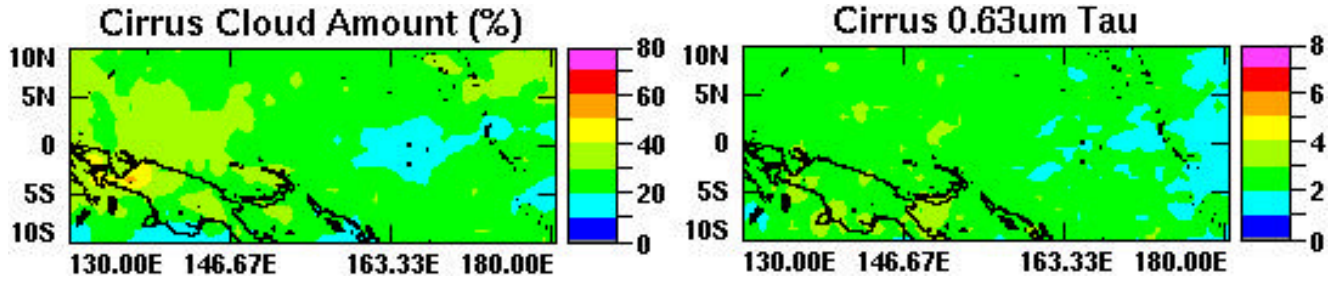

Figure 6. Mean high cloud parameters during Nauru99.

Mean cloud radiative forcings (CRF) are summarized in Figure 7. The LW CRF ranges up to 80 Wm^{-2}, while the SW CRF is as low as -80 Wm^{-2}. The largest magnitudes are found in the areas with the thickest highest cloud cover. Average LW and SW CRFs are 52.1 and -60.1 Wm^{-2}, respectively. When combined, the two CRF values yield mostly negative values with a mean of -8.0 Wm^{-2}. Thus, the clouds over the domain induce a net cooling of the earth-atmosphere.

Comparisons of the 24-hr satellite-derived cloud amounts with surface observations on Nauru are shown in Figure 8 for the entire IOP and for the large triangulation period. During the night (0600 - 2000 UTC) and early morning hours (2000 - 2400 UTC) for the entire IOP, the satellite-derived cloud amounts are consistently higher than the surface-based cloud observations. During the remainder of the day, the satellite cloud amounts are in close agreement with the WSI and MPL data. The radar detects fewer clouds during the daytime and more during the night compared to the ceilometer. The WSI is not used at night. Cloud fraction from the MPL is approximately 5 percent less than the GMS results during the night. The comparisons yield much different results during the triangulation period (Figure 8b). During the afternoon, the satellite analysis produces much lower cloud amounts than all of the sensors. At night, the GMS and radar cloud amounts are in close agreement and exceed the ceilometer values. The ceilometer and WSI results are nearly identical during the early morning hours.

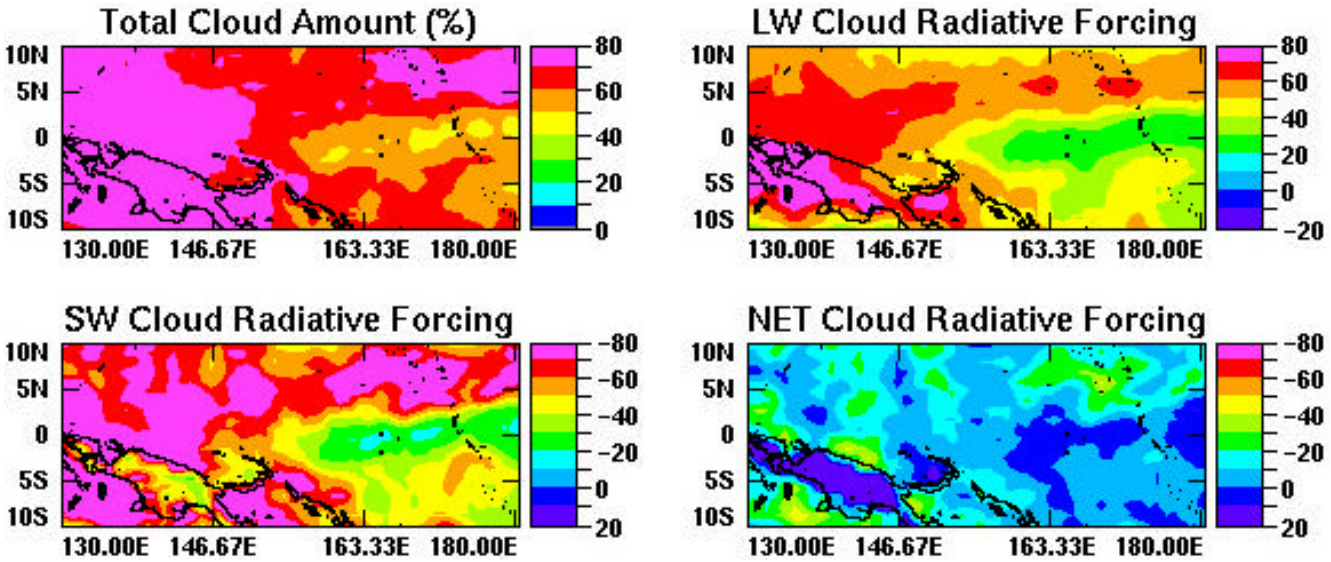

Figure 7. Mean cloud radiative forcing derived from GMS-5 during Nauru99.

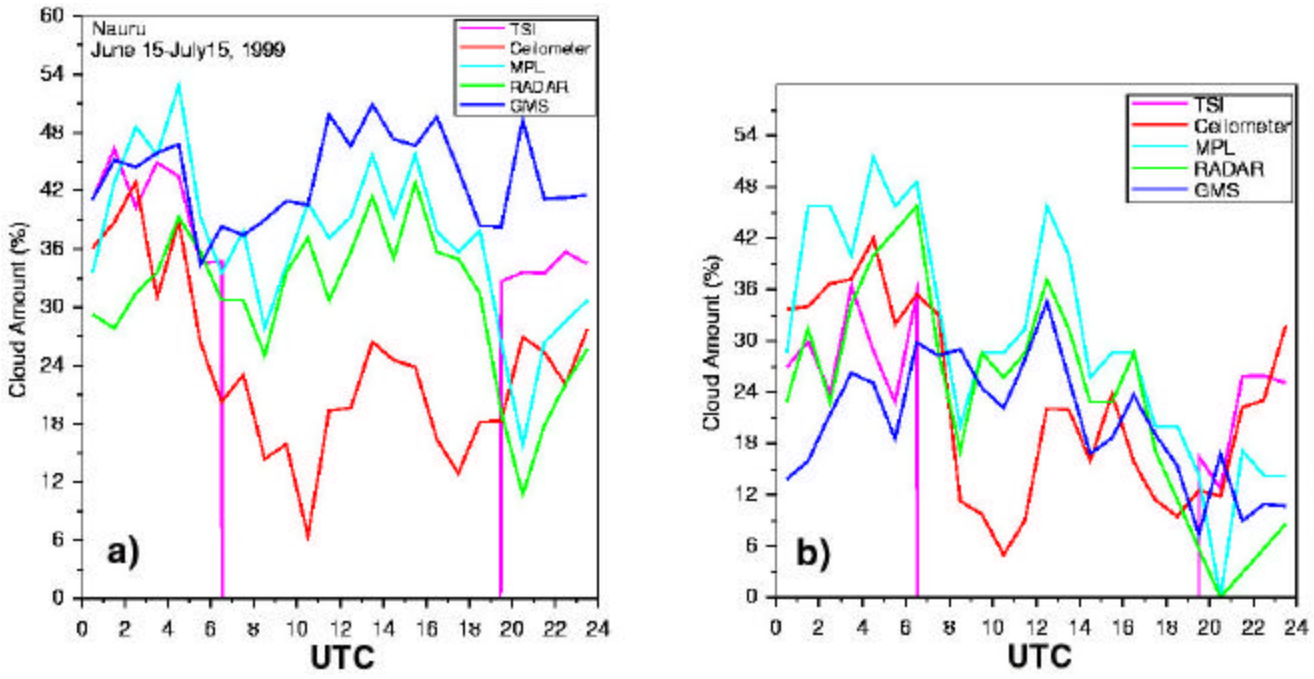

Figure 8. Comparison of satellite-derived cloud amounts with surface instruments during a) entire Nauru99 IOP and b) large triangulation period.

Discussion

For the most part, the cloud amounts from the satellite are in reasonable agreement with the surface observations. Each of the surface systems measures cloud fraction in a different manner with different sensitivities and areal coverage. The three active sensors all measure the presence of clouds directly

overhead. The ceilometer is limited in altitude to approximately 4 km. Thus, it is probably a good indicator of low clouds. The radar can detect clouds at various altitudes so it is good for identifying multi-layered systems. However, it is sometimes insensitive to very thin cirrus clouds composed of small particles. The MPL is sensitive to all clouds and is most accurate at night when no sunlight is superimposed on the return signal. The WSI obtains an estimate of cloud fraction over the hemispheric dome, but its spatial coverage is variable depending on the structure of cloud field. Thus, very low clouds will reduce the field of view while a scene containing only high clouds could represent a very extensive area when viewed by the WSI. These instruments are located on the west side of the island and may be biased during the daytime by a heat-generated cloud plume that forms each day and extends westward over the site (Nordeen et al. 2001). The satellite data represent an area of ~30 x 30 km nominally centered over the island. Because of navigation uncertainties, the analysis box may be centered on an area 7 km away from the island. Thus, there may be some mismatches between the surface and satellite.

The results in Figure 8 may reflect some of the site characteristics and the navigation errors. The ceilometer shows a buildup of low clouds beginning early in the morning and peaking around local noon (~0100 UTC) in both figures. A secondary peak occurs near midnight. All other surface instruments detect this systematic development but also record additional cloudiness which, given Figures 1 and 6, is presumably mostly thin cirrus. Most of the low cloud development over the site is the cloud plume while the high clouds are not related to the island in particular. Thus, in Figure 8, the satellite may be detecting low clouds over the surrounding island in addition to the plume over the island as well as the thin cirrus clouds resulting in a larger cloud fraction from the satellite compared to the other sensors for the entire IOP. Given the much better agreement for the whole period, the large differences during the large triangulation period are likely a result of the poor navigation. It may require an entire month of data to average out the navigation biases. It is not clear why the radar and MPL obtain smaller cloud amounts during the early morning compared to the ceilometer and WSI.

The cloud optical depths and albedos as well as CRF depend on the accuracy of the cloud amounts, calibration, and the clear-sky fluxes. The narrowband calibration appears to be accurate to better than 5 percent for ocean surfaces, but a different calibration may be necessary for land surfaces because of the large width of the GMS-5 VIS spectral band (0.5 - 1.0 µm). The calibration between GMS and VIRS was performed only over water where the spectral width, like that for clouds, has minimal impact because of the relatively flat spectral reflectance of water. More than half of the GMS VIS filter band is in the near infrared where vegetation reflectance is 3 or 4 times greater than in the visible band (0.5 - 0.7 µm), but the narrowband-broadband correlations were performed using an earlier GMS VIS channel that had a nominal spectral band of 0.55 - 0.75 µm. Thus, the GMS-5 reflectance over clear land is much greater than expected for the narrower VIS band on the old GMS imagers. The impact of this difference on the albedos and the optical depths needs further study. As noted earlier, some regions within the domain may have been persistently cloudy and thus may yield overestimates of clear-sky albedo. This overestimate would reduce the magnitude of the SW CRF and increase the net CRF. More accurate values of clear-sky albedo and temperature are needed to improve the accuracy of the CRF. Techniques are being developed to solve this problem.

Summary and Future Research

The LBTM was used here to retrieve cloud properties over the TWP for modeling and validation studies and to establish the context for the measurements made at the ARM surface sites. The results cover a large area with a high temporal resolution. These data are available online for use by the ARM science team and the general scientific community. Several areas for improvement have been identified and will be implemented and tested prior to full application of the method to more than 4 years of GMS data. These proposed improvements include more accurate clear-sky albedos and temperatures, separate calibrations and analyses for land and water pixels, and use of the GMS 12-μm channel to discriminate thin cirrus from low clouds at night. ECMWF sea surface temperatures will be used to improve the ocean IR thresholds and larger area estimates of clear albedos will be used to raise the accuracy of the CRF. Additional comparisons with surface observations over the ARM site at Manus Island and from the research ships, *Mirai* and *Ronald H. Brown*, during Nauru99 will help determine the robustness of the GMS retrievals and to understand the island-ocean differences in cloud amounts. Direct comparisons with fluxes from the Clouds and Earth's Radiant Energy System Project will be used to validate and improve the determination of fluxes from GMS. When the changes have been implemented, the GMS-based climatology will be processed and made available.

Acknowledgements

This research was supported by U.S. Department of Energy Interagency Agreement DE-A102-97ER62341 and by ITF No. 214216-A-Q1 from the Pacific Northwest National Laboratory.

Corresponding Author

Dr. Patrick Minnis, p.minnis@larc.nasa.gov, (757) 864-5671

References

Doelling, D. R., P. Minnis, R. Palikonda, J. K. Ayers, T. P. Ackerman, J. D. Spinhirne, and C. M. R. Platt, 1996: Validation of Satellite-Derived Cloud Properties during TOGA/COARE. In *12th Intl. Conf. on Clouds and Precipitation Proceedings - Volume 2*, August 19-23, 1996, Zurich, Switzerland, pp. 1281-1284.

Minnis, P., W. L. Smith, Jr., D. P. Garber, J. K. Ayers, and D. R. Doelling, 1995: Cloud properties derived from GOES-7 for the spring 1994 ARM Intensive Observing Period using Version 1.0.0 of the ARM Satellite Data Analysis Program. *NASA RP 1366*, August, p. 59.

Nguyen, L., P. Minnis, J. K. Ayers, W. L. Smith, Jr., and S. P. Ho, 1999: Intercalibration of geostationary and polar satellite data using AVHRR, VIRS, and ATSR-2 data. In *Proc. AMS 10th Conf. Atmos. Rad.*, June 28 - July 2, 1999, Madison, Wisconsin, pp. 405-408.

Nordeen, M. L., P. Minnis, D. R. Doelling, D. Pethick, and L. Nguyen, 2001: Satellite observations of cloud plumes generated by Nauru. *Geophys. Res. Lett.*, **28**, 631-634.